

Ab Initio MO Study of the Mechanism of Oxidation of Disulfides by Hydrogen Peroxide

Rois Benassi,* Luca G. Fiandri, and Ferdinando Taddei

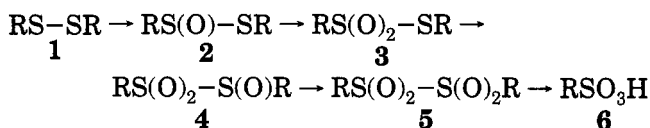
Dipartimento di Chimica, Università, Via Campi 183, 41100 Modena, Italy

Received March 28, 1995*

A theoretical study of the mechanism of the first oxidation step of disulfides to thiosulfonates was performed on hydrogen disulfide and methyl disulfide with hydrogen peroxide. *Ab initio* molecular orbital calculations were carried out with the 6-31G** basis set. Key equilibrium geometries and transition states were optimized at the MP2 level. The reaction paths were checked in accordance with the Intrinsic Reaction Coordinate (IRC) model to and fro along the reaction coordinate. The reaction turned out to be a two-step process: the first step is a high-barrier 1,2-hydrogen shift involving hydrogen peroxide to yield water oxide. The second step is a low-barrier oxygen shift to one of the sulfur atoms. Of the molecular complexes found between the reagents the most stable was a six-membered ring with two hydrogen bonds. Different activated complexes involving hydrogen disulfide in the formation of water oxide and corresponding to first-order saddle points were located. They correspond to transition states lower than that occurring in the isolated molecule of hydrogen peroxide. The lowest transition state is the result of an intermolecular proton exchange between hydrogen peroxide and hydrogen disulfide, which acts as a catalyst for the process. The formation of molecular complexes along the reaction path indicates the selectivity of the nucleophilic attack of one of the lone pairs of the sulfur atom on the oxygen atom. In the asymmetrically-substituted disulfide, the reaction mechanism is very similar to that found for the simple disulfide. The attack on the sulfur atoms is regioselective; oxidation of the most nucleophilic sulfur atom bonded to the methyl group is strongly preferred.

Introduction

Organic sulfides can be readily oxidized to the corresponding sulfoxides by peroxyacids, hydroperoxides, and hydrogen peroxide in a variety of solvents.¹ Oxidation of disulfides **1** leads ultimately to sulfonic acids **6**, but a number of stable intermediates (**2–5**) can be formed. The oxidation conditions can be controlled in order to increase the yield of intermediates, as reported by Allen *et al.*³



We focused our attention on the oxidation mechanism in the step from compounds **1** to compounds **2**. Dihydrodisulfide and methyl disulfide were chosen as models for experimental results obtained using more complex substrates such as, for example, methyl phenyl disulfide.⁴

Even though natural thiosulfonates are not necessarily formed from oxidation of the corresponding disulfides, this represents the most direct method for synthesizing these molecules.⁵ The chemistry of the disulfide bond has been widely reviewed in chemical and biochemical literature;² that of thiosulfonates, on the other hand, has only attracted attention since the isolation of allicin⁶ from cut garlic cloves. More recent papers have dealt with the

biological activities of compounds **2**,⁷ in view of their antitumor,⁸ antiviral,⁹ and antioxidant¹⁰ properties.

The oxidation mechanism of atoms bearing lone pairs of electrons, such as sulfur,¹¹ is still a matter for debate, and despite the availability of large amounts of experimental data there have been few theoretical studies dealing with their interpretation. It has been suggested¹² that the oxidation mechanism of organic sulfides may occur through an initial nucleophilic attack by a lone pair of the sulfur atom on one oxygen atom of the peroxy acid. The role of the oxidizing agent also has to be cleared up. A theoretical study of the mechanism of oxygen atom transfer from hydroperoxides has been recently reported.¹³

It would appear from the large amount of available data on the kinetics of the process that the oxidation of asymmetrical disulfides takes place mainly at the more electron-rich sulfur atom, although a very bulky sub-

(7) Kato, A.; Numata, M. *Tetrahedron Lett.* **1972**, 203. Yanagawa, H.; Kato, T.; Kitahara, Y. *Tetrahedron Lett.* **1973**, 1173.

(8) Kametani, T.; Fukumoto, K.; Umezawa, S. *Yakugaku Kenkyuu* **1959**, 31, 60; **1959**, 31, 132; **1960**, 33, 125. Weisberger, A. S.; Pensky, J. *Cancer Res.* **1958**, 18, 10. Weisberger, A. S.; Pensky, J. *Science* **1957**, 126, 1112. Hirsh, A. F.; Piantadori, C.; Irvin, J. L. *J. Med. Chem.* **1965**, 8, 10.

(9) Cavallito, C. J.; Buck, J. S.; Suter, C. M. *J. Am. Chem. Soc.* **1944**, 66, 1952. Wills, E. D. *Biochem. J.* **1956**, 63, 514.

(10) Barnard, D.; Bateman, L.; Cole, E. R.; Cunneen, J. I. *Chem. Ind. (London)* **1958**, 918. Bernard, D.; Bateman, L.; Cain, M. E.; Colclough, J.; Cunneen, J. I. *J. Chem. Soc.* **1961**, 5339. Bateman, L.; Cain, M.; Colclough, J.; Cunneen, J. I. *J. Chem. Soc.* **1962**, 3570. Rahman, A.; Williams, A. *J. Chem. Soc. B* **1970**, 1391. Cunneen, J. I.; Lee, D. F. *J. Appl. Polym. Sci.* **1964**, 8, 699.

(11) McDouall, J. J. W. *J. Org. Chem.* **1992**, 57, 2861.

(12) Davies, A. G. *Organic Peroxides*; Butterworth & Co., Ltd.: London, 1961; Chapter 9. Edwards, J. O. In *Peroxide Reaction Mechanisms*; Edwards, J. O., Ed.; Interscience Publishers, Inc.: New York, 1960; p 67. Behrman, E. J.; Edwards, J. O. *Progr. Phys. Org. Chem.* **1967**, 4, 93.

(13) Bach, R. D.; Owensby, A. L.; Gonzales, C.; Schlegel, H. B.; McDouall, J. J. W. *J. Am. Chem. Soc.* **1991**, 113, 6001.

* Abstract published in *Advance ACS Abstracts*, August 15, 1995.

(1) Savage, W. E.; MacLaren, J. A. In *The Chemistry of Organic Sulfur Compounds*; Kharasch, N.; Meyers, C. N., Eds.; Pergamon Press: Oxford, 1966; Vol. 2.

(2) Field, L. In *Organic Chemistry of Sulfur*; Oae, S., Ed.; Plenum Press: New York and London, 1977; pp 303–382.

(3) Allen, P., Jr.; Book, J. W. *J. Org. Chem.* **1962**, 27, 1019.

(4) Oae, S.; Takata, T.; Kim, Y. H. *Bull. Chem. Soc. Jpn.* **1982**, 55, 2484.

(5) Block, E. *Angew. Chem., Int. Ed. Engl.* **1992**, 31, 1135.

(6) Cavallito, C. J.; Bailey, J. H. *J. Am. Chem. Soc.* **1944**, 66, 1950.

Table 1. Optimized Geometries (Å, deg) and Zero-Point Vibrational Energies (ZPV, kcal/mol) at the MP2/6-31G** Level^a

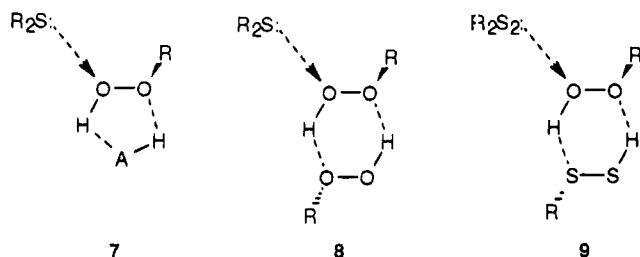
molecule	R(2,1)	R(3,2)	R(4,1)	R(4,2)	R(5,1)	θ(3,2,1)	θ(4,1,2)	θ(4,2,1)	θ(5,1,2)	τ(4,1,2,3)	τ(4,2,1,3)	τ(5,1,2,3)	ZPV
H ₂ O ₂ -H ₂ S	0.961 (0.957 ^b)	0.961 (0.957 ^b)				103.9 (104.5 ^b)							13.74 (12.88 ^c)
H ₄ -O ₁ -O ₂ -H ₃	1.466 (1.464 ^d)	0.968 (0.965 ^d)	0.968 (0.965 ^d)			98.65 (99.4 ^d)	98.65 (99.4 ^d)			120.27 (111.83 ^d)			16.74 (16.25 ^c)
O ₁ -O ₂ (H ₃)(H ₄)	1.519	0.967		0.967		100.92		100.92			250.48		16.97
TS1	1.577 ^e	0.971 ^e		1.013 ^e		98.46 ^e		63.32 ^e			104.26 ^e		14.88 ^e
H ₄ -S ₁ -S ₂ -H ₃	2.069 (2.055 ^f) (2.056 ^g)	1.333 (1.327 ^f) (1.327 ^f)		1.333 (1.327 ^f)		98.66 (91.3 ^f) (98.06 ^g)		98.66 (91.3 ^f) (98.06 ^g)			90.43 (90.6 ^f) (90.34 ^g)		12.15 (11.16 ^e)
(H ₃)C ₄ -S ₁ -S ₂ -H ₃	2.062 (2.038 ^h) (2.022 ⁱ)	1.335 (1.810 ^h) (1.806 ⁱ)	1.808 (1.810 ^h) (1.806 ⁱ)			99.18 (102.8 ^h) (104.1 ⁱ)	101.84 (102.8 ^h) (104.1 ⁱ)			87.38 (84.7 ^h) (83.9 ⁱ)			
H ₃ -S ₁ -S ₂ (O ₄)-H ₃	2.156			1.489	1.332			114.06	114.06			163.65	14.95
(H ₃)C ₅ -S ₁ -S ₂ (O ₄)-H ₃	2.130 (2.108 ^j)			1.493 (1.457 ^j)	1.810 (1.771 ^j)			113.37 (111.3 ^j)	95.65 (93.1 ^j)			171.43	

^a Experimental values are reported in parentheses. ^b Reference 17. ^c Reference 18. ^d Reference 19. ^e Transition state for the process H₂O₂ → OOH₂. ^f Reference 20. ^g Reference 21. ^h Referring to CH₃SSCH₃: ref 22. ⁱ Referring to CH₃SSCH₃: ref 23. ^j Referring to p-CH₃C₆H₄S(O)SC₆H₄-p-CH₃: ref 24.

stituent can sometimes change the direction of oxidation.⁴ Through our study of the oxidation of methyl disulfide, we intend, therefore, to verify the electrophilic character of the oxygen of water oxide when it is involved in a selective oxidation of the molecule's two sulfur atoms, which have different electron density.

Oxidation of methyl phenyl disulfide with hydrogen peroxide is performed in glacial acetic acid at room temperature;⁴ the solvent plays an important role in stabilizing the structure of the transition state. It has been suggested, on the basis of kinetic studies on the oxidation of sulfides by *tert*-butyl hydroperoxide,¹⁴ that a cyclic activated complex **7** is formed in a protic solvent. In the absence of a protic solvent, a second molecule of H₂O₂ may take part¹⁴ in the formation of the 6-membered cyclic activated complex **8**. A particular aim of this research was to clarify the role of the hydrogen disulfide molecule in stabilizing a transition state of type **9**, similar to **8**.

The model chosen for the oxidation reaction refers to a gas-phase process, and the role of solvents is not taken into account. A discussion of solvent effects is attempted.

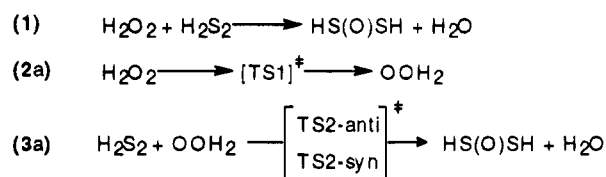


Computational Method

All calculations were carried out with the GAUSSIAN 92 series of programs.¹⁵ The 6-31G** basis set, which includes both d orbitals on heavy atoms and p orbitals on hydrogens, was used throughout.

Equilibrium and transition-state structures were fully optimized at the restricted Hartree-Fock (RHF) level and subsequently refined using the second-order Moller-Plesset perturbation theory (MP2). All correlation calculations used the full orbital space. Transition states were determined by means of frequency analysis at the RHF/6-31G** and MP2/6-31G** levels and are first-order saddle points. Each transition state was verified by following the only mode with an imaginary frequency to and from along the reaction coordinate in accordance with the intrinsic reaction coordinate (IRC) model

Scheme 1



at the RHF/6-31G** level. The evolution of geometries along the reaction path affords information about the reaction mechanism.

Zero-point vibrational energies were computed for equilibrium and transition structures. A natural bond orbitals (NBO) population analysis¹⁶ was carried out in order to examine the attack of the peroxide oxygen on the sulfur atom in terms of localized bond orbitals and lone pairs.

Results and Discussion

Optimized structures at the MP2/6-31G** level are reported in Table 1. The comparison between calculated and available experimental data shows that the *ab initio* values reproduce the experimental geometries reasonably well. The largest discrepancy is in the value of the torsional angle in hydrogen peroxide, where an angle closer to the experimental value was obtained with larger basis sets and higher-order corrections for electron correlation.²⁵ The calculated values of ZPE (zero-point vibrational energy) also agree well with experimental data.

(14) Dankleff, M. A. P.; Curci, R.; Edwards, J. O.; Pyun, H.-Y. *J. Am. Chem. Soc.* **1968**, *90*, 3209.

(15) GAUSSIAN 92, Revision C: Frish, M. J.; Trucks, G. W.; Head-Gordon, M.; Gill, P. M. W.; Wong, M. W.; Foresman, J. B.; Johnson, B. G.; Schlegel, H. B.; Robb, M. A.; Repogle, E. S.; Gomberts, R.; Andres, J. L.; Raghavachari, K.; Binkley, J. S.; Gonzales, C.; Martin, R. L.; Fox, D. J.; Defrees, D. J.; Baker, J.; Stewart, J. J. P.; Pople, J. A. Gaussian, Inc., Pittsburgh, PA, 1992.

(16) Reed, A. E.; Curtiss, L. A.; Weinhold, F. *Chem. Rev.* **1988**, *88*, 899.

(17) Benedict, W. S.; Gailar, N.; Plyler, E. K. *J. Chem. Phys.* **1956**, *24*, 1139.

(18) Shimanouchi, T. *J. Phys. Chem. Ref. Data* **1977**, *6* (3).

(19) Koput, J. J. *Mol. Spectrosc.* **1986**, *115*, 411.

(20) Winnemisser, G.; Winnemisser, M.; Gordy, W. *J. Chem. Phys.* **1968**, *49*, 3465.

(21) Hahn, J.; Schmidt, P.; Reinartz, K.; Behrend, J. *Z. Naturforsch., Teil B* **1991**, *1338*.

(22) Sutter, D.; Dreizler, H.; Rudolph, H. D. *Z. Naturforsch., A* **1965**, *20*, 1676.

(23) Beagley, B.; McAloon, K. T. *Trans. Faraday Soc.* **1971**, *67*, 3216.

(24) Kiers, C.; Vos, A. *Recl. Trav. Chim. Pays-Bas* **1978**, *97*, 166.

(25) Carpenter, J. E.; Weinhold, F. *J. Phys. Chem.* **1986**, *90*, 6405; **1988**, *92*, 4295; **1988**, *92*, 4306.

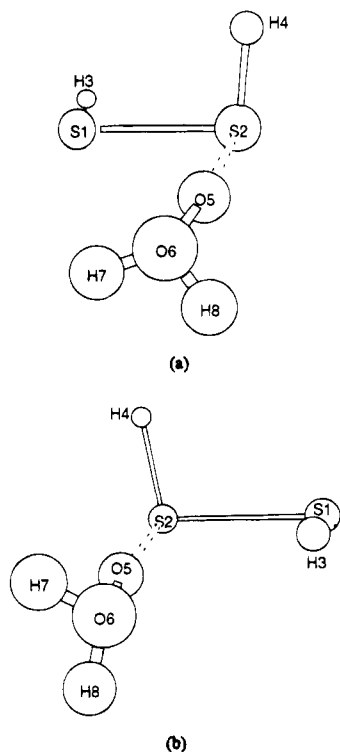


Figure 1. Structures of the transition states TS2-anti (a) and TS2-syn (b), respectively, at the RHF/6-31G** level.

In an attempt to establish the mechanism by which disulfides oxidize to yield thiosulfates, we set out to identify a first-order saddle point for reaction 1 (Scheme 1). The simultaneous transfer of an oxygen atom from H_2O_2 to H_2S_2 would involve both a 1,2 hydrogen shift and a simultaneous oxygen shift, due to the cleavage of the O—O bond. However, the attempt to find such a transition state failed. This led us to look for a two-step process, represented by reactions 2a and 3a in Scheme 1. Similarly, the gas-phase oxidation of ammonia¹³ with hydrogen peroxide was interpreted as a two-step process led by a 1,2 hydrogen shift and followed by a facile $\text{S}_\text{N}2$ -like displacement (*ca.* 2.0 kcal/mol barrier). It is assumed that the oxygen atom is donated by water oxide, since oxygen transfer requires a low activation barrier.¹³

Scanning the energy hypersurface for the above reactions, we located a transition state TS1 for reaction 2a (Table 1), corresponding to the 1,2 hydrogen shift that yields water oxide, and two activated complexes, corresponding to two different sites of attack by water oxide

on the sulfur atom, reaction 3a. These transition states were checked by an IRC (intrinsic reaction coordinate) calculation²⁶ at the RHF/6-31G** level, and it was observed that the shortening of the O··S bond coincides with the increase in the O—O bondlength of water oxide. In each TS2 (Figure 1) the oxygen atom (O_5) lies in the plane defined by the S,S,H atoms of the disulfide, on the same side as H with respect to the S—S bond (TS2-syn) or opposite side to H (TS2-anti). The energetics of the two steps of the oxidation reaction are summarized in Table 2: only energy values calculated at the MP2/6-31G** level are reported. The highest activation energy is required for the hydrogen shift in the hydroperoxide, reaction 2a, as in the case of the oxidation of ammonia.¹³ The oxygen transfer requires a low activation energy only for the anti attack, the syn process thus being preferred. The overall oxidation is found to be strongly exoergic.

The attack of the sulfur atom on the oxygen atom of water oxide was described by natural bond orbital (NBO) analysis.¹⁶ Each sulfur atom has two different lone pairs (*lp1* and *lp2*), the former (*lp1*) with 70% s character and 30% p character, the latter (*lp2*) being a pure p orbital. The directionality of the lone pairs, with $\text{S}_1\text{—S}_2$ as the z axis (S_1 at the origin) is reported in Table 3 as a function of the polar coordinates θ and ϕ . The direction of bond formation between the oxygen and sulfur atoms ($\text{O}_5\text{—S}_2$ in Table 3) and the structures of the transition states (TS2-syn/anti) enable the lone-pair directly involved to be identified. This orbital turns out to be *lp2*, almost entirely of p character. The attempt to find a transition state in which the attack on the oxygen atom occurs along the direction of the second (in plane) lone pair failed.

When IRC calculations are performed along the reaction coordinate for oxygen transfer, energy values are found which are lower than those of the reagents, water oxide and hydrogen disulfide. This led us to look for formation, along the reaction path, of bimolecular complexes of the type observed in the study of the reaction of water oxide with water and ammonia.¹³ The participation of disulfide in these molecular complexes could affect the complete reaction profile (Scheme 2). This is equivalent to considering H_2S_2 both as a single "solvent" molecule in a gas phase process behaving as a homogeneous catalyst and as a nucleophilic reagent.

When the energy hypersurface for the reaction was scanned, noncovalent complexes were located (Figure 2). I is considered to be the molecular complex in the entrance channel of the first step of the complete reaction.

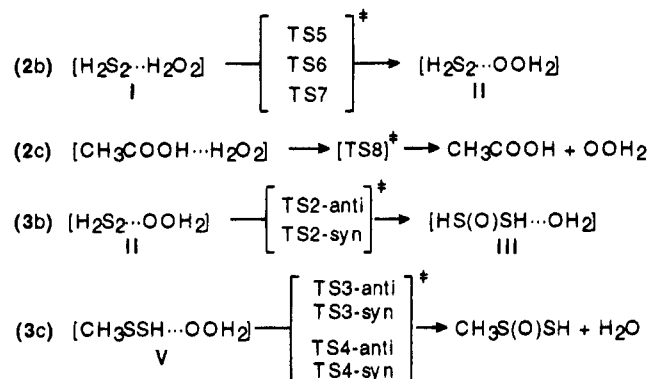
Table 2. Energy^a of Activation and of Reaction (from Left to Right) for Reactions Reported in Schemes 1 and 2 Calculated at MP2/6-31G**//MP2/6-31G**

reaction	reagents/TS/products	ΔE^*	ΔE
1	$\text{H}_2\text{O}_2, \text{H}_2\text{S}_2/\text{H}_2\text{S}_2\text{O}, \text{H}_2\text{O}$		−30.4 (−30.6) ^b
2a	$\text{H}_2\text{O}_2/\text{TS1}/\text{OOH}_2$	58.9	53.4 (53.6)
3a	$\text{OOH}_2, \text{H}_2\text{S}_2/\text{TS2-anti}/\text{HS(O)SH}, \text{H}_2\text{O}$	0.7 (1.0)	−83.8 (−84.2)
2b	TS2-syn	−1.1 (−0.8)	
	complex I/TS5/complex II	49.0	44.0
	TS6	53.1	
	TS7	56.8	
2c	$[\text{AcOH} \cdots \text{H}_2\text{O}_2]/\text{TS8}/\text{AcOH}, \text{OOH}_2$	23.7 ^c	
3b	complex II/TS2-anti/complex III	16.2 (15.3)	−78.5 (−77.9)
3c	TS2-syn	14.4 (13.5)	
	complex V/TS3-anti/ $\text{CH}_3\text{S(O)SH}, \text{H}_2\text{O}$	19.6	−64.7
	TS3-syn	17.4	
	TS4-anti	16.5	
	TS4-syn	15.2	

^a Values expressed in kcal/mol. ^b Values in parentheses are corrected for ZPV energy. ^c Calculated at MP2/6-31G**//RHF/6-31G** level.

Table 3. Orientation of the Two Lone Pairs of Sulfur in H_2S_2 Compared with the Direction of the Attack $\text{O}_5 \cdots \text{S}_2$

	$lp1^a$		$lp2^a$		$\text{O}_5 \cdots \text{S}_2$ (TS2-syn)		$\text{O}_5 \cdots \text{S}_2$ (TS2-anti)	
	θ (deg)	ϕ (deg)	θ (deg)	ϕ (deg)	θ (deg)	ϕ (deg)	θ (deg)	ϕ (deg)
RHF	55.7	199.3	87.6	93.5	88.8	97.0	88.0	94.0
MP2	55.3	193.5	88.4	92.2	92.3	101.5	97.1	97.1

^a Values refer to S_2 .**Scheme 2**

Two hydrogen bonds can be identified in this structure (i.e., $\text{O}-\text{H} \cdots \text{S}$ and $\text{S}-\text{H} \cdots \text{O}$) which is similar to the most stable one reported by Dobado *et al.*²⁷ for the hydrogen peroxide dimer (HPD). The second minimum (II) is a six-membered ring complex between one molecule of H_2S_2 and OOH_2 , whose structure shows a higher degree of planarity than in I. IRC calculations show that returning from TS2 we find II, which can be considered to be the most stabilized structure leading to the second transition state. Lastly, the third minimum (III) corresponds to a linear structure with a single highly energetic hydrogen bond ($\text{O}-\text{H} \cdots \text{O}$) between one molecule of thiosulfinate and one of water and which appears to be the bound system in the exit channel of the second step of the complete reaction. Figure 3 enables a comparison to be made between the reaction profiles both taking into account and ignoring the formation of such complexes (Figure 3b and a, respectively).

The binding energies for these noncovalent complexes were calculated as the difference between the energy of the supersystem and the sum of the energies of the separated molecules. The values are reported in Table 4. Corrections for the basis set superposition error (BSSE)²⁸ were attempted by adopting the FCP (full function counter poise) method.^{28b} The weight of the BSSE corrections is significant, especially at the correlation energy level (ranging from 39% to 53% of ΔE), a conclusion also reached for HPD.²⁷

In order to gain further insight into the electronic interactions characterizing these complexes we performed a natural bond orbital (NBO) analysis within the donor-acceptor model based on localized orbitals.¹⁶ The most stabilizing noncovalent interactions determined for each complex are reported in Table 5. In this table Σ_{tot} is the sum of all intermolecular interactions obtained by suppressing all the mixed Fock matrix elements between molecule 1 and molecule 2 and then recalculating the

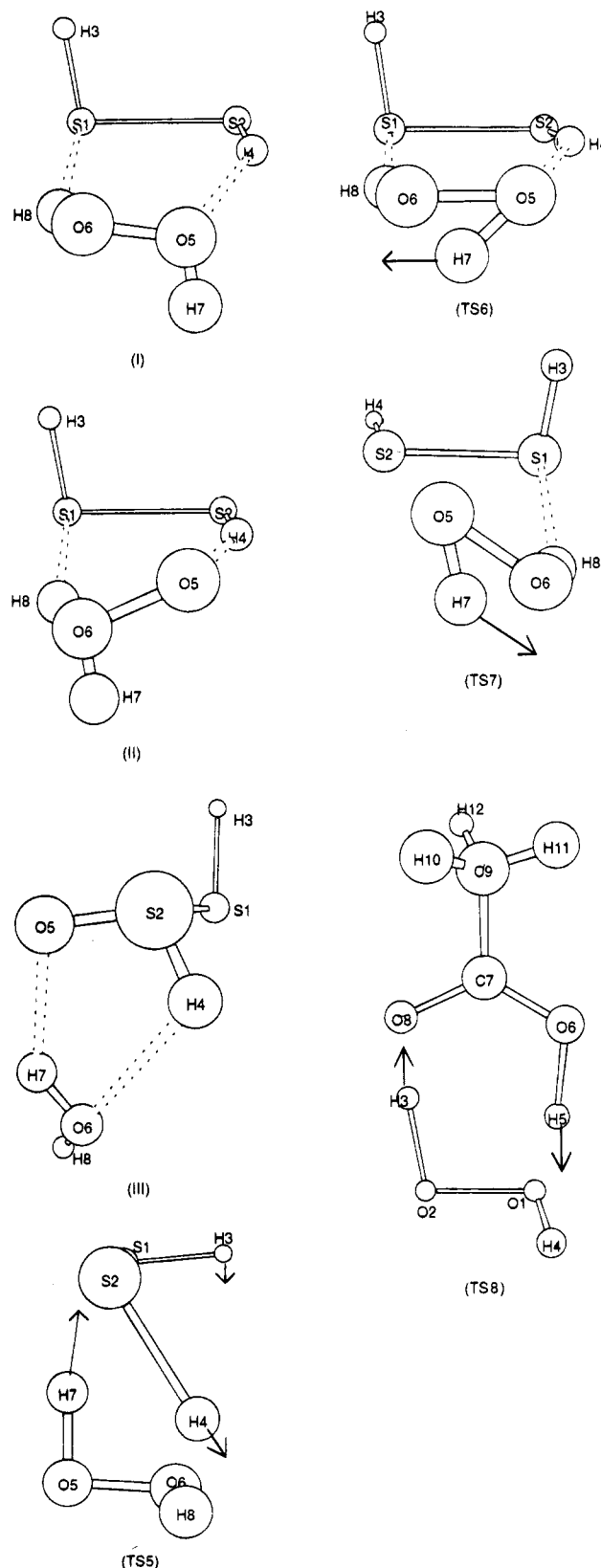


Figure 2. Structures of the noncovalent complexes (I, II, and III) and of TS5, TS6, TS7, and TS8, respectively, calculated at the RHF/6-31G** level. The arrows indicate the main components of the transition vectors.

total energy. Complexes I and II are mostly stabilized by the two hydrogen bonds, while for III other noncovalent interactions become important, as can be seen from the percentage of hydrogen bond contribution (66%) to the total noncovalent energy. Even if the Σ_{tot} values

(26) Gonzalez, C.; Schlegel, H. B. *J. Phys. Chem.* **1988**, *90*, 2154.(27) Dobado, J. A.; Molina, J. M. *J. Phys. Chem.* **1993**, *97*, 7499.(28) (a) Clementi, E. *J. Phys. Chem.* **1962**, *36*, 750. (b) Boys, S. F.; Bernardi, F. *Mol. Phys.* **1970**, *19*, 553.

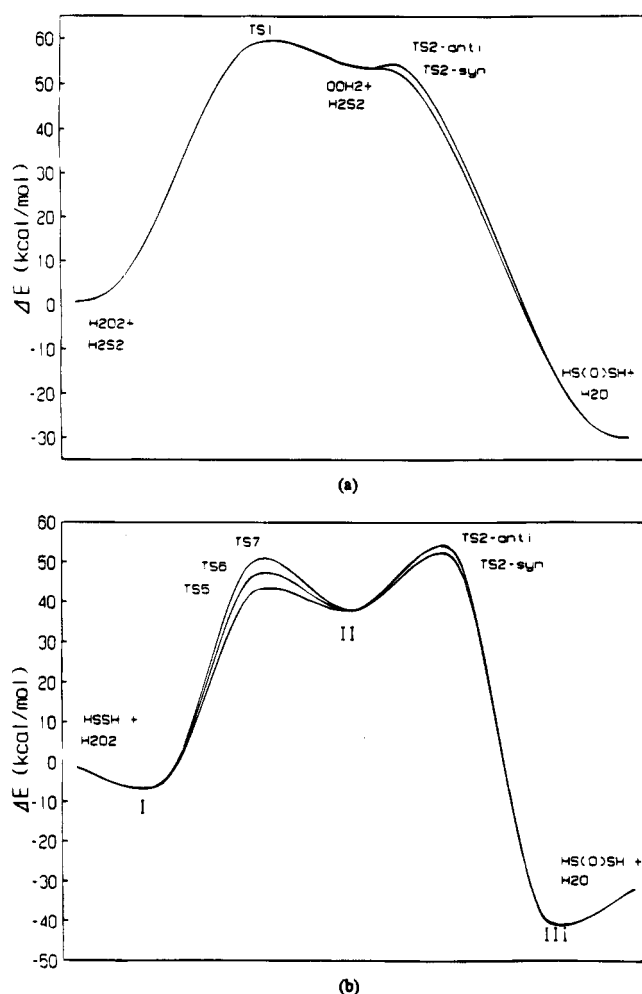


Figure 3. Reaction paths calculated at the MP2/6-31G** level for the oxidation of dihydrodisulfide with hydrogen peroxide: (a) energy surfaces without formation of molecular complexes; (b) effect of the formation of molecular complexes on the reaction path.

Table 4. Binding Energies (kcal/mol) ΔE for Noncovalent Complexes I–III Appearing in Scheme 2

complex	I ^a [H ₂ S ₂ ··H ₂ O ₂]		II ^b [H ₂ S ₂ ··OOH ₂]		III ^c [HS(O)SH··OH ₂]	
	RHF	MP2	RHF	MP2	RHF	MP2
ΔE^{ncd}	-3.44 (-4.0)	-6.00 (-7.3)	-7.25 (-8.7)	-15.48 (-18.6)	-8.27 (-8.1)	-10.13 (-10.1)
BSSE	0.88	2.67	1.76	6.1	2.62	5.35
ΔE^{ccd}	-2.6	-3.3	-5.5	-9.4	-5.6	-4.8

^{a-c} Values in parentheses refer to complexes IV, V, and VI in that order. ^d nc and cc are noncorrected and FCP corrected values, respectively, for basis set superposition error (BSSE).

cannot be compared with the binding energies, they show the same qualitative trend, as can be seen by comparing Σ_{tot} and ΔE^{cc} in Table 5. The complex showing the highest stabilization is II, as expected from the polar character of the O–O bond in water oxide.¹³ The oxygen atom in OOH₂ (O₅) has three lone pairs, which, in the NBO representation, are *lp1* (30% s/70% p), *lp2* (100% p) and *lp3* (70% s/30% p). These lone pairs interact with the $\sigma^*(S_2-H_4)$ (9.3 kcal/mol), while *lp2* of S₁ interacts significantly with $\sigma^*(O_6-H_8)$ (10.1 in II vs 3.4 kcal/mol in I).

The formation of the above-mentioned complexes determines the energy profile of the reaction as reported in Figure 3b. The apparent negative activation barrier

Table 5. Most Significant Noncovalent Interactions (kcal/mol) Calculated According to the Natural Bond Order (NBO) Analysis

complex	I ^a	II ^b	III ^c
<i>lp1</i> (S ₁) → $\sigma^*(O_6-H_8)$	0.74 (0.92)	0.81 (1.52)	
<i>lp2</i> (S ₁) → $\sigma^*(O_6-H_8)$	3.41 (4.60)	10.08 (14.0)	
<i>lp1</i> (O ₅) → $\sigma^*(S_2-H_4)$	1.24 (1.30)	0.25 (0.34)	
<i>lp2</i> (O ₅) → $\sigma^*(S_2-H_4)$	1.50 (0.98)	0.30 (–)	
<i>lp3</i> (O ₅) → $\sigma^*(S_2-H_4)$		9.32 (6.25)	
<i>lp1</i> (O ₄) → $\sigma^*(O_6-H_7)$			3.27 (3.55)
<i>lp2</i> (O ₄) → $\sigma^*(O_6-H_7)$			4.57 (4.91)
Σ	7.0 (7.8)	20.8 (22.1)	7.8 (8.5)
Σ_{tot}	7.3	19.2	11.9
%	94	~100	66
$-\Delta E^{ccd}$	3.3	9.4	4.8

^{a-c} Values in parentheses refer to IV, V, and VI in that order. These are the complexes formed in the corresponding reaction involving CH₃SSH. ^d Binding energies at MP2/6-31G**//MP2/6-31G** level from Table 4.

calculated at the MP2/6-31G** level to reach the TS2-syn transition state (Figure 3a) disappears. In regard to the directionality of attack, the syn direction seems to be slightly preferred, TS2-syn being ~2.0 kcal/mol lower than TS2-anti.

The different nucleophilic character of the sulfur atoms should lead to regioselective oxidation of asymmetrically-substituted disulfides. To verify this we examined the oxidation of CH₃SSH with OOH₂. Along the reaction path, we found complexes like those occurring in the reaction of hydrogen disulfide (IV, V, VI, respectively), while the structure of the six-membered ring complex (V) between CH₃SSH and OOH₂ was seen to be very similar to that of II. The attack of water oxide on methyl disulfide involved four transition states, corresponding to the approach of the oxygen atom to the two different sulfur atoms from the syn and anti directions. TS3/TS4 led to an attack on the sulfur atom bonded to H/CH₃, respectively (reaction 3c, Scheme 2). The energy values reported in Table 2 show that the preferred syn attack is maintained in the oxidation of methyl disulfide. As expected from experimental results,⁴ the sulfur atom bonded to the methyl group is oxidized more easily than that bonded to the hydrogen atom, and the character of electrophilicity assigned to the oxidation reaction is satisfied.

The possible participation of a molecule of H₂S₂ in the mechanism of the 1,2 hydrogen shift was also investigated. Three different transition states (reaction 2b, Scheme 2), corresponding to possible 1,2 hydrogen migrations, were located and checked with IRC calculations to and fro from the saddle-points at the RHF/6-31G** level. The corresponding activated complexes are reported in Figure 2. TS5 and TS6 have cyclic structures with a five- and six-membered ring, respectively; TS7 is linear with one hydrogen bond. The calculated activation energies for the three processes are reported in Table 2, where I is the common ground state for the three reaction paths.

The activation barrier for the 1,2 hydrogen shift through TS5 is consistently lower (by almost 10 kcal/mol at the MP2/6-31G** level) than without the participation of H₂S₂. IRC calculations show the behavior of hydrogen disulfide to be that of a bifunctional catalyst. Intermolecular proton exchange occurs between sulfur and oxygen atoms in order to release water oxide for the oxygen transfer to H₂S₂. In TS6 and TS7, H₂S₂ participation does not involve intermolecular hydrogen transfer.

The oxidation of methyl phenyl disulfide with H_2O_2 is usually performed in glacial acetic acid at room temperature.⁴ A molecule of a strong proton-donating species such as acetic acid should stabilize the transition state for the 1,2 hydrogen shift in hydrogen peroxide. The noncovalent, seven-membered cyclic complex in the entrance channel of the reaction has a binding energy of -15.1 kcal/mol at the MP2/6-31G** level. The transition state for hydrogen migration (reaction 2c, Scheme 2) corresponds to TS8 in Figure 2. As can be seen from Table 2, the participation of a molecule of AcOH greatly lowers the activation barrier for the forward reaction.

Analysis of the single mode with an imaginary frequency shows that acetic acid clearly behaves as a bifunctional catalyst. In other words, in addition to its typical action as a solvent, acetic acid also exhibits a marked ability to decrease the activation energy of the 1,2 hydrogen shift in hydrogen peroxide by a proton-exchange mechanism.

Acknowledgment. Financial support from the Italian Government (Ministero Università e Ricerca Scientifica) is warmly acknowledged.

JO9506084